An Investigation into Self Sustained Activity within a Sparsely Connected Hierarchical Network of Limit Cycle Oscillators in the Incoherent State

Bachelor Thesis in Physics

Faculty of Science

University of Potsdam

Jonas Beck
Student Number: 783710

Tübingen, 15 October 2019

Supervisor and Primary Examiner: Dr. Ralf Toenjes
Secondary Examiner: Dr. Udo Schwarz

Deutsche Zusammenfassung

In dieser Arbeit simuliere ich, mit Hilfe numerischer Methoden, ein Netzwerk identischer, unidirektionaler, Grenzzyklusoszillatoren, die in einem spärlich verbundenen, hierachischem Netzwerk angeordnet sind und in ihrem asynchronen Zustand gehalten werden. Durch das Treiben ausgewählter Elemente mit einem Ornstein-Uhlenbeck-Prozess kontrolliere ich dann die quasistochastische Bewegung aller Oszillatoren, indem ich die Parameter der treibenden Prozesse variiere.

Das Ausrechnen der Autokorrelationsfunktionen für jeden Oszillator und der Vergleich dieser mit einer Brownschen Zufallsbewegung auf dem Kreis, lässt mich dann die Difussions- und Zeitkonstanten für die Bewegung jedes Oszillators bestimmen. Diese werden dann wiederum benutzt um die Entwicklung des chaotischen Phasendiffussionsprozesses durch das Netzwerk zu verfolgen und dessen stationären Punkt für 3 verschiedene Verbindungsdichten zu ermitteln. Die Parameter die diesen chaotischen Phasendiffusionsprozess charakterisieren werden zudem für jede Netzwerksschicht visualisiert und eine sorgfälltige Approximation für Diffusions- und Zeitkonstante am Fixpunkt werden bestimmt.

Außerdem werden das generelle Verhalten des Netzwerks im Bezug auf seinen geordneten und seinen ungeordneten Zustand diskutiert.

Abstract

In this thesis I perform numerical simulations on a set of identical unidirectionally coupled limit cycle oscillators arranged in a sparsely connected hierarchical network, that is held in its asynchronous state. Driving a selected number of units with an Ornstein-Uhlenbeck process I control the quasi stochastic motion of all the individual units in the network, by varying the parameters of the driving noise.

After calculating the autocorrelation function for each oscillator and comparing them to a Brownian flight on a circle I will then determine the diffusion constants and scattering rates for each oscillator. These are used to track the evolution of the chaotic phase diffusion process through the network and to establish its stationary point for 3 different sets of connection densities. I visualise the parameters characterising the chaotic phase diffusion process throughout the layers of the network and give a thorough estimate for the scattering rate and diffusion constant at the fixed point.

In addition I discuss the general behaviour of this network with regards to its ordered and disordered state.

Contents

1 Introduction

Large oscillatory networks, such as in the brain[1], often tend to take on collective behaviours e.g. global waves, global oscillations and other synchronous activities[2]. However, in some cases, depending on the properties of the network and its oscillators, asynchronous activity without clear spatial patterns may also emerge[3][4][5]. In theory, this state is especially favourable for systems with a high degree of heterogeneity, since a state of complete synchronisation might not be reached in them, even though asymptotically it is the most stable[6][7]. However, contrary to the first intuition, even if oscillators are identical and the coupling tends to decrease phase differences, for random networks with uncorrelated and homogeneously distributed node degrees the network may still enter a quasi-stationary asynchronous state[8]. In this state, units behave quasi-stochastically, as they are being driven by a large number of other (likewise quasi-stochastic) units and the correlation statistics of the driving, i.e., the network noise, is connected to the statistics of the single unit in a self-consistent manner[9]. Although spatial correlations in this state are negligible, the temporal correlations can be distinctive and their understanding could reveal a lot about the nature of the chaotic phase diffusion processes happening inside the network. A theory of the asynchronous state therefore involves determining the autocorrelations of the single units and the total network noise[9]. However, so far these temporal correlations and their relation to the network and its units have remained an open question within the study of these systems.

One way to study this problem is by introducing a known external stochastic process that drives selected units. A moderation of the networks internal noise can be then achieved by varying parameters of the driving noise. Comparing aspects of the driving noise to those of the networks internal noise, makes it possible to study the relation between these processes, as units coupled to a driving process must realise a version of that same process[8]. By submitting the external units to Brownian motion, the behaviour of the internal units can be approximated by the same constants governing the motion of the external units, namely their diffusivity and scattering rates. Those can be determined

and then related to that of the driving process.

With the help of this scheme the meanfields of k complex oscillators were coupled to an Ornstein-Uhlenbeck process. A comparison of the diffusion constants of the coupled process to the actual diffusion constant of the oscillators, indicated the existence of a unique stationary phase diffusion process characterising the incoherent state[8]. This indication of a unique stationary diffusion process prompts the question as to whether this kind of self sustained activity also exists for other kinds of networks, how it is affected by the driving noise and as to how it might be characterised.

With this work, I therefore aim to contribute to the ongoing research effort in the area of self sustained activity in the incoherent state. I set out to investigate the question posed above by exploring the autocorrelations of meanfields and individual units in the layers of a sparsely connected hierarchical network of limit-cycle oscillators. By comparing the internal network noise to Brownian motion on a circle, I will estimate its scattering rate and diffusivity and observe their evolution through the layers of the network. Mapping this to the external driving process, I set out to determine the fixed point of the system, describe how it is reached and visualise its evolution through the network. Furthermore, I will explore how changes made to the topology of the network affect it.

To achieve these goals, I will write a program that recreates the system described above as accurately as possible. I will then perform numerical simulations, calculating the autocorrelations of the individual units in the process. By fitting a the correlation function of Brownian flight on a circle to the measured correlations, I will extract the diffusion constants and scattering rates of the underlying phase diffusion processes. Finally, these will be used to characterise the chaotic phase diffusion processes across the network and as to how it compares to the outside driving process.

2 Theoretical Background

2.1 The System

The system that I investigate can be thought of as sparsely connected hierarchical network of identical and weakly coupled limit-cycle oscillators. The structure of the network is comprised of layers of oscillators, the $0th$ of which will be fed with noise, provided by an appropriately scaled Ornstein-Uhlenbeck process. For consistency throughout this work, I will start indexing at 0, as this will be how it is implemented computationally later on. For the purpose of improved clarity I will be dividing the system into 3 parts, addressing

- the structure of the network,
- the model used for the oscillator lattice,
- the noise that is driving the system,

separately. Having derived a complete model of the underlying physical system, I will then talk about the types of phase dynamics inherent to the system and the diffusion process that I will try to investigate in this thesis.

2.1.1 The Network

The oscillators are arranged in a network structure that can be described as a sparsely connected hierarchical graph. The "backbone" of this network structure consists of N_L linear, L long chains of unidirectionally coupled oscillators. To this structure random unidirectional connections are added, with origin (i_k, j) and destination $(i_l, j+1)$, where i_k and i_l are referring to different chains and j to a segment on that chain. That means a given oscillator in a chain segment makes a random connection to one of the oscillators in the next chain segment on another chain. This results in a structure similar to what can be seen in Fig. 2.1a. where the linear chains (dark blue connections) are broken up by random cross connections (light blue). However, rather than talking about a set of N_L cross linked linear chains, for easier understanding and convenience purposes, I will be describing the topology of the network in terms of a set of L layers, each containing N_L nodes. This is also how the graph

in Fig. 2.1a was numbered and will be analysed later. Thus, the network can be described as follows: Every node (i_n, j) in a given layer l receives exactly one connection from the "directly adjacent node" $(i_n, j-1)$ in the previous layer $l-1$ and a constant prespecified number k_{cross} of other incoming connections from random nodes $(i_m, j-1)$ within that same previous layer $l-1$. This is true for all layers where $l > 0$. This leads to a uniform degree distribution σ_{in} and thus a homogeneous network, which will be important later.

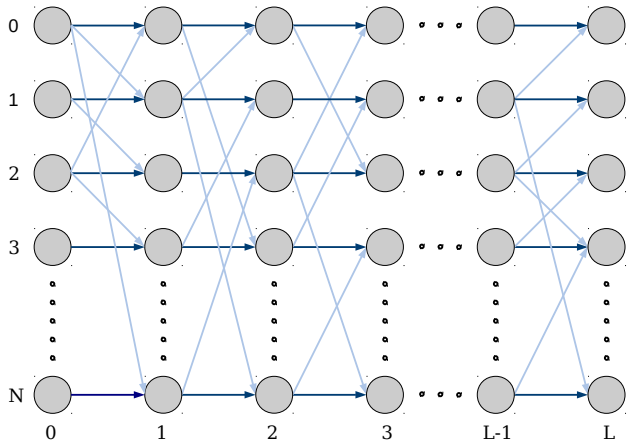

(a) Graph of the network structure, with nodes indexed by layer and chain membership.

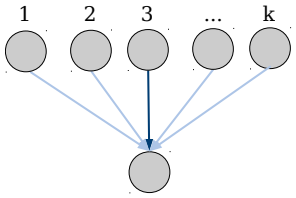

(b) Example graph for a single node, with incoming neighbouring (→) and cross connections (→).

Since the connections are unidirectional in nature, the relevance of the outgoing connections on a given note is diminished. When describing the network I will therefore only consider the incoming connections on every node. The number of total incoming connections per node k_{in} is dependent on the number of incoming cross connections k_{cross} (Fig. 2.1a →) such that $k_{in} = 1 + k_{cross}$ per node (see Fig. 2.1b). This way the density of connections within the network is constant $\sigma_{in} = 1 + \sigma_{cross} = 1 + k_{cross}$. Alongside N_L and L this is the third parameter characterising the network. Every node therefore has a prespecified maximum number of incoming connections. This leads to a total number in overall connections of $N_{connections} = N_L \cdot (L-1) \cdot k_{in}$.

Representing the connections within the network can be done in the form of a matrix H, where $H_{ij} \neq 0$ if there is a connection from node i to node j. There are $N_L \cdot L$ oscillators in total, leading to $(N_L \cdot L)^2$ possible connections. The coupling matrix must therefore be of $dim(H) = (N_L \cdot L) \times (N_L \cdot L)$ to potentially allow for all of these connections to be realised. Applying what we know about the networks structure to H, only a simple set of rules is needed to represent the network in this form. For a given connection from

any node i where $\{i \in \mathbb{N} \mid 0 < i < N_L \cdot L - 1\}$ to any other node j where $\{j \in \mathbb{N} \mid 0 < j < N_L \cdot L - 1\}$ must then be true:

1. All coupling is unidirectional and no oscillator can connect to itself. The matrix must therefore be of triangular form. That means $H_{ij} = 0$ if $i \leq j$, where $\{(i,j) \in \mathbb{N}^2 \mid 0 < i < (N_L \cdot L - 1) \wedge 0 < j < (N_L \cdot L - 1)\}$.

2. Every node i_l has a direct neighbour in the previous layer i_{l-1}. Therefore $H_{ij} > 0$ for $i = j + (N_L - 1)$ and $i \geq N_L$.

3. Lastly, every node has a fixed number of incoming connections from random nodes in the previous layer, that are not the results of case 2. This leads to k_{cross} cases, where $H_{ij} > 0$, if $(i,j) \neq (i, i - (N_L - 1)) \wedge \left\lfloor \frac{i}{N_L} \right\rfloor - 1 = \left\lfloor \frac{j}{N_L} \right\rfloor$.

An example of the matrix with $N_l = 3$, $L = 3$ and $k_{in} = 2$ can be seen in Fig.(2.1a). The bold numbers represent connections made to immediate neighbours and the lighter numbers the ones made to random nodes in the next layer (see connections $\rightarrow$ and $\rightarrow$ in Fig. 2.1a for comparison). Note that H is not normalised.

$$
\begin{array}{cc|ccc|ccc|ccc}
 & \text{l:} & \multicolumn{3}{c|}{0} & \multicolumn{3}{c|}{1} & \multicolumn{3}{c}{2} \\
 & \text{n:} & 0 & 1 & 2 & 0 & 1 & 2 & 0 & 1 & 2 \\
\hline
0 & 0 & 0 & 0 & 0 & 0 & 0 & 0 & 0 & 0 & 0 \\
 & 1 & 0 & 0 & 0 & 0 & 0 & 0 & 0 & 0 & 0 \\
 & 2 & 0 & 0 & 0 & 0 & 0 & 0 & 0 & 0 & 0 \\
\hline
1 & 0 & \mathbf{1} & 0 & 1 & 0 & 0 & 0 & 0 & 0 & 0 \\
 & 1 & 0 & \mathbf{1} & 1 & 0 & 0 & 0 & 0 & 0 & 0 \\
 & 2 & 0 & 1 & \mathbf{1} & 0 & 0 & 0 & 0 & 0 & 0 \\
\hline
2 & 0 & 0 & 0 & 0 & \mathbf{1} & 0 & 1 & 0 & 0 & 0 \\
 & 1 & 0 & 0 & 0 & 1 & \mathbf{1} & 0 & 0 & 0 & 0 \\
 & 2 & 0 & 0 & 0 & 0 & 1 & \mathbf{1} & 0 & 0 & 0
\end{array}
$$

Figure 2.2: Matrix representation of the network graph, with the bold numbers representing neighbouring connections and the lighter numbers random cross connections.

2.1.2 The Model

In this next section I will go into more depth about how I intend to model the dynamics of the oscillators within the network I described above.

As this thesis is heavily inspired by previous work done on the "synchronisation transition of identical phase oscillators in a directed small-world network"[8],

for comparability of results I opt to use the same model[2][10], that was used in this paper. The interaction of the nodes and the emerging phase dynamics of my system are therefore best described by the same adapted set of phase equations. These model the phase dynamics of a number of identical, weakly coupled limit-cycle oscillators in a corotating frame of reference where the common oscillator frequency is zero and coupling is weakly anharmonic and diffusive. The equations are therefore in line with the assumptions[10] made by the original model and a solid choice to describe the problem with.

In the following few paragraphs I will derive the full set of equations from the most simple case of the Kuramoto phase equations (Eq. 2.1).

$$\frac{d\theta_i}{dt} = \omega_i + \frac{\epsilon}{N}\sum_{j=1}^{N} g(\Delta\theta_{ij}), \qquad i = 1 \dots N \tag{2.1}$$

Here $g(\Delta\theta_{ij})$ represents the coupling function, ϵ the coupling strength, N the number of oscillators, ω_i the natural frequency of a given oscillator and θ_i its current phase.

The coupling function (Eq. 2.2) we will use, serves as a good approximation for diffusive coupling in weakly anharmonic oscillators[11], with $g(0) = 0$ and $g'(0) > 0$. This leads to interactions depending sinusoidally on the phase difference between pairs of oscillators.

$$g(\Delta\theta) = \sin(\Delta\theta - \alpha) + \sin(\alpha) \tag{2.2}$$

The constant $\alpha(-\pi/2 < \alpha < \pi/2)$ provokes the emergence of unusual effects[6][10] and makes the coupling function a more realistic approximation to coupled limit-cycle oscillators[12], as it sways the balance of the coupling function away from 0. Due to invariance of Eq. 2.1 and Eq. 2.2 under transformation $\alpha \to -\alpha$ and $\theta_i \to -\theta_i$, $\alpha(0 \leq \alpha \leq \pi/2)$ suffices as the parameter range[8]. This choice of coupling function also has the convenience, that it allows for a later transformation and subsequent simplification of the system.

However, before simplification, we have to note, that the model in Eq. 2.1 assumes global, all-to-all coupling of oscillators with different natural frequencies. In contrast my implementation is dependent on the topology of the network, while the oscillators are all the same. After a short rearranging of the equation, this property can be made use of by setting natural frequencies $\omega_i = \omega$ and with a subsequent transformation into a corotating reference frame

$(\omega + \epsilon \sin(\alpha)) \to 0$. This can be seen below (Eq. 2.5).

$$\frac{d\theta_i}{dt} = \omega_i + \frac{\epsilon}{N} \sum_{j=1}^{N} \sin(\theta_j - \theta_i - \alpha) + \sin(\alpha) \tag{2.3}$$

$$= (\omega + \epsilon \sin(\alpha)) + \frac{\epsilon}{N} \sum_{j=1}^{N} \sin(\theta_j - \theta_i - \alpha) \tag{2.4}$$

$$= \frac{\epsilon}{N} \sum_{j=1}^{N} \sin(\theta_j - \theta_i - \alpha), \qquad i = 1 \dots N \tag{2.5}$$

The topology of the network can be addressed by replacing the coupling term $\frac{\epsilon}{N}$ with a coupling matrix H_{ij} that takes into account the structure of the network. Here, more selective control over the coupling is possible and makes it possible to "insert" the structure of the network into the equations. This means the system can now be represented in terms of Eq. 2.6.

$$\dot{\theta}_i = \sum_{j=1}^{N} H_{ij} \sin(\theta_j - \theta_i - \alpha), \qquad i = 1 \dots N \tag{2.6}$$

with $H_{ij} \geq 0$ being the coupling matrix. $H_{ij} > 0$ if node i is connected to node j and $H_{ij} = 0$ if that is not the case. We assume uniform and normalised input strength for every individual oscillator, leading to $H_{ij} = 1/k_i^{in}$ and subsequently

$$\sum_{j=1}^{N} H_{ij} = 1. \tag{2.7}$$

This prevents bias of phase velocities towards nodes with a higher number of incoming connections or in the case of higher asymmetry α [12][8]. Furthermore, phase velocities are bounded, i.e. $-1 \leq \dot{\theta}_i - \sin(\alpha) \leq 1$, due to the normalisation.

As was mentioned in an above part of this section, the choice of the coupling function makes further refinement of the equations possible. First, the coupling function can be thought of as being complex, with $\sin(\theta_j - \theta_i - \alpha)$ representing just the imaginary part. This means equation 2.6 can be rewritten as

$$\dot{\theta}_i = \sum_j H_{ij} Im[e^{i(\theta_j - \theta_i - \alpha)}] = Im\left[\sum_j H_{ij} e^{i(\theta_j - \theta_i - \alpha)}\right]. \tag{2.8}$$

Now, let us define the complex local meanfield of those oscillators as,

$$\Psi_i = \sum_j H_{ij} z_j = r_i e^{i\Theta_i}. \tag{2.9}$$

Substituting Eq. 2.9 into Eq. 2.8 we are able to successfully uncouple the system of differential equations. Which leaves us with the expression in Eq. 2.10.

$$\dot{\theta}_i = Im[r_i e^{i(\Theta_i - \theta_i - \alpha)}] = Im[z^* \Psi_i e^{-i\alpha}] \tag{2.10}$$

The final step now is to treat θ_i as the phase of the complex oscillator $z_i = e^{i\theta_i}$ and describe its velocity by

$$\dot{z}_i = \frac{d}{dt} e^{i\theta} = \frac{d\theta}{dt} \frac{d}{d\theta} e^{i\theta} = i\dot{\theta} z. \tag{2.11}$$

If Eq. 2.10 is then inserted into Eq. 2.11, we get a description of each oscillators complex dynamics

$$\dot{z}_i = iIm[z_i^* \Psi_i e^{-i\alpha}] z_i = r_i i Im[e^{i(\Theta_i - \theta_i - \alpha)}] z_i. \tag{2.12}$$

The state of every oscillator is therefore fully determined by the asymmetry parameter α, its momentary phase θ_i and its local meanfield, namely its phase Θ_i and magnitude r_i.

2.1.3 The Driving Noise

The $0th$ layer of the network, has so far received no input of any kind, as the coupling is unidirectional and the $0th$ layer is not connected to any other layer of oscillators, apart from the subsequent one. That means, the network would not swing at all in this configuration, as Eq. 2.10 would be 0 due to $\Psi_i = 0$ for nodes in the $0th$ layer. To prevent this from happening, nodes in this layer will be "repurposed" to provide nodes in the following layer with their own changing local meanfield, in order to drive them and all subsequent nodes in the chains.

We recall, that for a given oscillator the change in the complex state over time $\dot{z}_i$ is subject to a surrounding meanfield Ψ_i according to Eq. 2.12. Therefore, driving the oscillators within the whole network is as simple as providing a local meanfield $\Psi_i \neq 0$ to oscillators in the $1st$ layer. Since the local meanfield changes according to the sum of the incoming connections from oscillators

$z_i = e^{i\theta_j}$, it is sufficient to introduce a process according to which phases in the first layer change. The process can be as simple as subjecting each oscillator to Brownian motion, which can be described by the following stochastic differential equation (Eq. 2.13),

$$\dot{v}_\theta + \gamma v_\theta = \Gamma(t), \tag{2.13}$$

where v_θ denotes the velocity of an oscillator, γ the scattering rate and $\Gamma(t)$ a Langevin force with $\langle \Gamma(t) \rangle = 0$ and correlation function $\langle \Gamma(t+\tau)\Gamma(t) \rangle = q\delta(\tau)$ [13]. q determines the strength of the Langevin force and acts as a proportionality constant. Assuming $\Gamma(t)$ is Gaussian with mean zero and δ correlation, then Eq. 2.13 can be compared to the Ornstein-Uhlenbeck process,

$$dv_\theta = -\gamma v_\theta dt + \sigma dW(t) \tag{2.14}$$

Noting that $\frac{dW(t)}{dt} = \eta(t)$ is a normally distributed variable with $\eta \backsim \mathcal{N}(0, t)$, we are able to rewrite Eq. 2.13 as

$$\dot{v}_\theta = -\gamma v_\theta + \sqrt{2D}\eta(t). \tag{2.15}$$

Here, I used the fact that $q = \sigma^2 = 2D$ according to the Fokker-Planck equation [13], with D being the Diffusion coefficient. This way all the network dynamics are directly or indirectly dependent on the constants D and γ.

The noise in Eq. 2.15 will be implemented to drive the $0th$ layer as follows: The phase of an oscillator in the $0th$ layer is made to change with a velocity v_i according to

$$\dot{\phi}_i = v_i, \tag{2.16}$$

$$\dot{v}_i = -\gamma v_i + \sqrt{2D}\eta(t). \tag{2.17}$$

This way oscillators beyond the $0th$ layer will now couple to multiple of these processes via Eq. 2.18 and thus start moving in a similar, quasi-stochastical manner according to the changing local meanfield Ψ_i, as ϕ_i changes according to v_i. Which is what we intend with this driving scheme.

$$\Psi_i = \sum_j^{k_{in}^i} e^{i\phi_j} \tag{2.18}$$

2.2 The Phase Diffusion Process

Now, with the model complete, let us consider the possible phase dynamics of the system at hand. Similar to the dynamics in a "directed small world network" [8] we expect the system to assume different dynamical states, characterisable through the order parameter of the meanfields $r(t) = \left|\frac{1}{N}\sum_i e^{i\theta_i(t)}\right|$. $r(t) \approx 1$ for a state of total synchronisation and $r(t) \approx 0$ for a state of asynchronicity. Even though synchronisation is the asymptotically favourable solution, the system can exist in a state well below $r(t) = 1$, depending on the densities of shortcuts σ_{cross} and the asymmetry α in the coupling function[8]. Due to the topological similarities between a "small world" and the hierarchical network, this means my system can be "forced" into an asynchronous state with low enough values of σ_{cross} and high enough values of α. I intend to exploit this property during my experiments, as I seek to investigate the phase diffusion in this nonsynchronous state.

However, as σ is varied, one has to be cautious, as the network makes a "topological crossover"[8] somewhere between values of low ($\sigma_{cross} < 1$) and high ($\sigma_{cross} > 1$) cross connection density σ_{cross}, which is also reflected in the phase dynamics. Here, the network transitions from being comprised mostly of linear chains, to consisting mainly of so called "joints" (see Fig. 2.1a). These are nodes that receive more than one incoming connection and thus cause a non linear interaction. Expectedly this will lead to behaviour without clear spatiotemporal patterns.

It is this chaotic regime that I seek to investigate further as part of my work. In particular, am I interested in the phase diffusion process that happens in this orderless regime and how it evolves through the layers of the network.

To repeatedly reach this state I will therefore ensure:

- densities of connections and a uniform distribution of them, such that $\sigma_{in} > 1$ in all cases. - As a side note: The network of joints is therefore also highly homogeneous.
- low enough densities of connections, such that $r(t) < 1$ at all times.
- high enough values of α, such that $r(t) < 1$ all the time.

2.2.1 Describing the Activity in the Incoherent State

Now, that we are aware of the possible types of behaviour in our network and know how the incoherent state can be reached, I will attempt to describe the motion within this state in more detail.

Here, some properties of our model come as a convenience. Firstly, the phase dynamics of each oscillator can be viewed as statistically equivalent due to the homogeneity of our model. Secondly, we can assume that an oscillator being coupled to k other independent and identically distributed phase diffusion processes via Eq. 2.12, is therefore bound to realise the same process. This, however, only holds in large unidirectional networks in the incoherent state[8]. This means we ought to be able to compare parameters of the ingoing noise to properties of the phase diffusion process deeper within a network that is large enough.

Recall, that Eq. 2.13 defines the change in velocity of oscillators within the $0th$ layer. Solving for the initial condition $v(t=0) = v_0$, we obtain Eq. 2.19 and subsequently the corresponding correlation function Eq. 2.21.

$$v(t) = v_0 e^{-\gamma t} + \int_0^t e^{-\gamma(t-t')}\Gamma(t')dt' \tag{2.19}$$

$$\langle v(t_1)v(t_2)\rangle = v_0^2 e^{-\gamma(t_1+t_2)} + \int_0^t e^{-\gamma(t_1+t_2-t_1'-t_2')} q\delta(t_1'-t_2')dt_1'dt_2' \tag{2.20}$$

$$\langle v(t_1)v(t_2)\rangle = v_0^2 e^{-\gamma(t_1+t_2)} + \frac{q}{2\gamma}\left(e^{-\gamma|t_1-t_2|} - e^{-\gamma(t_1+t_2)}\right) \tag{2.21}$$

For $t_1 = t_2$ we find the variance of the phase velocities of such a Brownian flight to be equal to $v^2 = \frac{q}{2\gamma} = \frac{D}{\gamma}$, which can be directly compared to the variance $var(\dot{\theta})$ of the chaotic phase diffusion process. However, since the variance of the phase velocities is not very easy to determine, we want to calculate the mean squared phase displacement at time t. Assuming $v(t=0) = v_0$ and $\phi(t=0) = \phi_0$, this can be expressed as

$$\left\langle(\phi(t)-\phi_0)^2\right\rangle = \left\langle\left[\int_0^t v(t_1)dt_1\right]^2\right\rangle = \left\langle\int_0^t v(t_1)dt_1\int_0^t v(t_2)dt_2\right\rangle \tag{2.22}$$

$$= \int_0^t\int_0^t \langle v(t_1)v(t_2)\rangle\, dt_1dt_2. \tag{2.23}$$

Substituting in Eq. 2.21 and integrating, leaves

$$\left\langle (\phi(t) - \phi_0)^2 \right\rangle = \left(v_0^2 - \frac{q}{2\gamma} \right) \frac{(1 - e^{-\gamma t})^2}{\gamma^2} + \frac{q}{\gamma^2} t - \frac{q}{\gamma^3}(1 - e^{-\gamma t}). \tag{2.24}$$

With the mean square displacement of the phases in the $0th$ layer, we can now begin to draw comparisons to the movement of the oscillators themselves, as these should also behave like subject to Brownian forces. More specifically that the autocorrelation functions of the individual units (Eq. 2.25) should be comparable to the autocorrelations of a Brownian process on a circle (Eq. 2.26), where W(t) represents such a process.

$$c(\tau) = \langle z_i^*(t + \tau) z_i(t) \rangle \tag{2.25}$$

$$c(\tau) = E\left[e^{iW_i(\tau)} \right] = \varphi_{W_i}(\tau) \tag{2.26}$$

Writing this out one realises, $c(\tau)$ resembles the characteristic function of the Gaussian distribution, which can be written out as,

$$N(\mu, \sigma^2) = e^{it\mu - \frac{1}{2}\sigma^2 t^2}, \tag{2.27}$$

for mean μ and variance σ^2. However, in our case, with a mean of zero and the variance of the phase displacement (Eq. 2.24), this can be expressed as

$$c(\tau) = exp\left(-\frac{q}{\gamma^2}\tau + \frac{q}{\gamma^3}(1 - e^{-\gamma\tau}) \right). \tag{2.28}$$

Substituting q = 2D according to the Langevin Force in Eq. 2.13 and considering only the real part of both the equations (Eq. 2.25, Eq. 2.26) then gives rise to the expression we're after.

$$\langle \cos(\theta_i(t + \tau) - \theta_i(t)) \rangle = exp\left(-\frac{D}{\gamma^2}\tau + \frac{D}{\gamma^3}(1 - e^{-\gamma\tau}) \right) \tag{2.29}$$

Here, we have already introduced the assumption that we start with a velocity distribution rather than a sharp value, where $< v_0^2 >= \frac{q}{2\gamma}$, causing the first term to vanish and also substituted in $q = 2D$.

From this circular autocorrelation function $c(\tau) = \langle \cos(\theta(t + \tau) - \theta(t)) \rangle$ we are now able to estimate effective phase diffusion constants D_z and the effective

scattering rates γ_z for oscillators well beyond the driving layer, by comparing it to the autocorrelation function of a Brownian flight on a circle (Eq. 2.29). This enables us to characterise each individual oscillator or ensemble of oscillators through their diffusion and scattering constants.

Describing the individual diffusion processes of the units within the network in this manner, accomplishes two things. Firstly, we are now able to characterise the average diffusion of entire ensembles e.g. each layer of oscillators. Secondly, and more importantly, it lets us compare the diffusion, e.g. D and γ of the external stochastic driving process to D and γ of the internal phase diffusion processes. This way, the effect of altering the driving noise can be studied.

2.2.2 Self Sustained Activity

After describing the asynchronous state in detail and deriving a way to characterise the diffusion processes in and outside of the network, we can focus now start discussing the unique stationary diffusion process that we expect to observe with our set up.

This means that whatever the parameters of the driving process are outside, the internal phase diffusion processes should converge towards a set of values for D and γ that act as the most stable solution for a given topology of the network or choice of coupling function. In this case, the topology refers primarily to the density of connections. Choosing the parameters of the driving process close enough to those of the stationary process, will cause the whole network to settle in this state and assume a pattern of so called 'self sustained activity'. The self sustained part of the term refers to the apparent stable fixed point of the phase diffusion process, while the activity part emphasises the asynchronous irregular behaviour that units in this state are exhibiting. This means the most stable state of the network in the incoherent regime is a state characterised by spontaneous activity and constant phase diffusion throughout the whole network.

This state of self sustained activity can therefore be identified easily, as it should prevail throughout the whole network. This means every oscillator or ensemble of oscillators should be characterisable by the same set of diffusion constants D and γ. In other words, the constants of diffusion will not change throughout the layers of the network. If we visualise this, we should be able to identify this stationary phase diffusion process quite trivially.

3 Method

In order to realise and simulate the system described above, I translated the system as (Sec. 2.1) into C++ code. I chose to use C++ for this, as it is fast and capable as well as being suited for numerical calculations, thanks to being a compiled language. Furthermore, the possibility to use optimisation flags such as -O3 reduces execution time significantly. Other benefits include low and high level programming functionality as well as the option to write object oriented code, which makes it easier to structure the whole project.

Similar to Sec. 2.1, I will split the following section about the implementation of the system into the same three subsections. I will address each one individually, though be it in a slightly different order.

3.1 The Implementation

For practical reasons and the purpose of clarity I first split the system into the same three distinct parts that I split Section 2.1 into. I then wrote a class for each. This enabled me to tamper with parts of the simulation without affecting other components. Furthermore, it allowed for multiple sets of networks, oscillators or driving conditions to be quickly evaluated, simply by creating new instances for parts of the system.

To aid processing speed and avoid the use of nested arrays, I decided to code matrices of $dim(M) = K \times K$ (where $K \in \mathbb{N}$), as a vector of $dim(V) = 1 \times K \cdot K$ and used a function to map the 2D coordinates (i,j) to a 1D index on this vector. However, for better understanding I will be ignoring this detail from here on, as the methods used are still valid regardless, only differing in the execution slightly.

3.1.1 The Network

The first class that I wrote was dedicated to the generation of the coupling network. The constructor of that class takes the number of oscillators per layer N_l, the number of layers L and the number of connections k_{in} each node

of the network shall receive. Rather than representing the connections as talked about in Sec. 2.1.1, we can exploit the sparse character of the matrix, by keeping a list for each node that contains its neighbours. This way, we transform the coupling matrix into a "next neighbour matrix" $\mathcal{NN}$, going from $dim(H) = N_L \cdot L \times N_L \cdot L$ to $dim(\mathcal{NN}) = N_L \cdot L \times k_{in}$. For the small k_{in} that we are dealing with, this is extremely favourable. A "next neighbour" representation means, that each index i of the vector $\mathcal{NN}$ holds a list containing the indices j_k of all neighbours that node i is receiving a connection from. In this way the amount of information that has to be stored is minimal. An example of this can be found in Fig. 3.1. The fact that some nodes (eg. in layers 0 & 1) have fewer than k_{in} incoming connections is coded as $\mathcal{NN}_{ij} = -1$. The -1 acts as a placeholder for a non existent neighbour and will be skipped during later processing. This way, $\mathcal{NN}$ can still be stored and interpreted as a $N_L \cdot L \times k_{in}$ matrix. The notation further has the convenience of simplifying the normalisation of H, as k_i^{in} can be determined by just counting the number of incoming neighbours, stored in $\mathcal{NN}_i$. $k_i^{in} = k_{in}$ for all i except for the $0th$ layer where $k_i^{in} = 0$ of course.

$$\mathcal{NN}_{ij} = \begin{bmatrix} -1 & -1 \\ -1 & -1 \\ -1 & -1 \\ 0 & 2 \\ 1 & 2 \\ 2 & 1 \\ 3 & 5 \\ 4 & 3 \\ 5 & 4 \end{bmatrix} \tag{3.1}$$

Therefore, all the information on the networks size and connections can be conveniently contained within the terms $\mathcal{NN}$, N_L and L. Fed with the parameters N_L, L and k_{in}, an instance of this class will be able to construct a network according to the parameters given and rules outlined in Sec. 2.1.1 and represent it in terms of $\mathcal{NN}$, N_L and L.

3.1.2 The Noise

The second class that I designed was concerned with the introduction of a noisy process to the system. This way, I can drive the first layer of oscillators in my network according to the scheme specified in Sec. 2.1.3. Provided with information about the dimensionality of the system $N_l \cdot L$, the scattering rate γ, the mean value μ for the Langevin force and the diffusion constant D, it ought to be able to generate and update a set of N_l values following the stochastic

differential equation (Eq. 2.14) of the Ornstein-Uhlenbeck process. However, for this to work, equation 2.14 has to be discretised.

For this purpose let us define a small $\epsilon > 0$ and represent Eq. 2.14 as

$$v(t_{N+1}) = v(t_N) + \epsilon \dot{v}(v_{t_N}, t_N) + \sqrt{2D} W^{\epsilon}(t_N). \tag{3.2}$$

We can then set $t = N\epsilon$ and $\tau = n\epsilon$ with $1 \ll n \ll N$. This leaves Eq. 3.3.

$$v(t+\tau) = v(t) + \sum_{i=N}^{N+n} \epsilon \dot{v}(v_{t_i}, t_i) + \sum_{i=N}^{N+n} \sqrt{2D} W^{\epsilon}(t_i) \tag{3.3}$$

However, since we can actually solve the homogeneous part of the differential equation, we can use its solution in place of the first term and by applying the central limit theorem to the second, the equation (see Eq. 3.4) can now be solved numerically by using a computer.

$$\dot{\theta}_{t+\tau} = v_{t+\tau} = v_t \cdot e^{-\gamma\tau} + \sqrt{2D\tau} \cdot n_\tau \tag{3.4}$$

Here, n_τ is a normally distributed variable, with $n_\tau \sim \mathcal{N}(0,1)$. Setting $\tau = dt$ gives an updated value for $\dot{\theta}$ based on the current velocity v_t in steps of dt.

Now, in order to integrate Eq. 3.4 and acquire the phase, that we need for Eq. 2.6, I employ the Euler Maruyama scheme[14]. This is a method integrate stochastic differential equations and approximates the true solution X is with a Markov chain Y and initial condition $Y_0 = x_0$. It can be defined through:

- the partitioned interval [0,T], where $0 = \tau_0 < \tau_1 < \cdots < \tau_N = T$ and $\Delta t = T/N$,
- the recursively defined Markov chain Y_n for $1 < n < N$, where $Y_{n+1} = Y_n + a(Y_n)\,\Delta t + b(Y_n)\,\Delta W_n$,
- and the i.i.d. random variables $\Delta W_n = W_{\tau_{n+1}} - W_{\tau_n}$.

This is the weakest iterative method for integration of stochastic differential equations, however, since the second term of our equation is not time dependent, terms of higher order (e.g. in the Milstein scheme) would vanish anyway, leaving just the first order term from the Euler scheme.

3.1.3 The Model

The model is realised through a translation of the equations in Sec. 2.1.2, mainly Eq. 2.6, into C++ code, however, with an important difference. Instead of relying on the coupling matrix H, as shown in the equations in Sec. 2.1.2, it will be replaced by the "next neighbour" matrix $\mathcal{NN}$, as discussed in Sec. 3.1.1. This way Eq. 2.6 can be rewritten as:

$$\dot{\theta}_i = \sum_{neighbours} \frac{1}{k_i^{in}} \sin(\theta_{neighbour} - \theta_i - \alpha). \tag{3.5}$$

Where the sum is taken over all neighbours of node i and normalised with factor $\frac{1}{k_i^{in}}$.

Now, that $\dot{\theta}_i$ can be determined for all $N \cdot L$ oscillators, including for those in the $0th$ layer (see Eq. 3.4), we shift focus to the approximation of the initial value problem at hand. The aim here is to estimate the time evolution of the system $\dot{\theta} = f(t, \theta)$ for a set of initial values $\theta(t_0) = \theta_0$. There exist a number of possible techniques to do this, however, as we're already limited by the precision of the first order Euler Method, which is used to calculate the phases in the $0th$ layer, there is no real gain to be made, from using higher order Runge-Kutta methods. I will therefore be using the classical Euler Method for integrating E.3.5. This means that the error per iteration will be on the order of $O(dt^2)$, causing the total cumulative error to be approximately $O(dt)$. If the computational hardware allows for it a small value for dt should therefore be chosen, which in my case will be on the order of $O(10^{-2})$.

After deciding on dt, the initial conditions need to be set. I chose to set $\theta_i(t_0) = \theta_{i,0}$ for all oscillators in the network to a random value, such that $\theta_i \in [0, 2\pi) \quad i = 0, ..., N \cdot L - 1$. One could also initialise all $\theta_i(t_0) = 0$, however, this would increase the transient time for the network to settle to an equilibrium state significantly.

Now, a numerical scheme can be specified, iteratively updating the values of t, θ_t and $\dot{\theta}_t$ according to $\dot{\theta} = f(t, \theta)$ within a finite time interval $t \in [0, T]$.

1. Partition the interval of t such that $t_n = t_0 + ndt$.
2. Update $\dot{\theta}_n = f(t_n, \theta_n)$.
3. Go from t_n to $t_{n+1} = t_n + dt$.

4. $\theta_{n+1} = \theta_n + dt \cdot \dot{\theta}_n$.

5. if $t < T$, jump back to 2.

From this triplet of values, all other important metrics can be derived, such as the local meanfields Ψ_i, the global meanfields of each layer Ψ_l and the corresponding autocorrelation functions $c_z(\tau)$,$c_l(\tau)$ of the individual units and layers.

3.1.4 Data Processing

The data gathered throughout the simulations eventually has to be analysed and visualised. In order to extract the constants γ and D, characterising the diffusion process, the real part of the measured autocorrelation functions $c_l(\tau)$ has to be fitted to the autocorrelation function for a Brownian flight on a circle (Eq. 2.28). To achieve this I used python and the scipy.optimze's curve_fit function, which optimises using the least square method[15]. For visualisation I employed matplotlib's pyplot library.

4 Results

In the following section I will present the results of my numerical simulations and describe my findings. With the help of the model that I have built up in the previous parts, I will then try to explain the behaviour of the oscillators in the incoherent state.

All simulations will be performed with an initial transient of 20,000 steps at a step size of dt = 0.01, randomly initialised phases. If not stated otherwise the observed time period will also include 20,000 steps. This means $t = N_{step} * dt = 20,000 \cdot 0.01 = 2000$

4.1 General System Behaviour

First, I will lay the groundwork for studying the unique stationary phase diffusion process in the incoherent state. This involves scoping out the parameter regions, where the oscillators can be found in the nonsynchronous state. We recall those parameters to be N,L and k_{in} for our network, α for the oscillators and D and γ for our driving process. As a measure of the incoherency I will use the mean value of the order $R =< r(t) >$ and I will consider the system to be asynchronous if $R < 0.5$.

I will skip looking at the effect of α, as a high value is related to high disorder[8] and therefore just fix α to its maximum value $\alpha = \frac{\pi}{2}$. Furthermore, increasing the networks depth L will have no impact on the asynchronicity of a given layer since the network is unidirectional. However, it should be noted that later layers tend to increase in order, which means the networks depth will always be chosen, such that the last layer can still be considered asynchronous. Simulating any additional layers, would be computationally wasteful.

The first thing I will be looking at, is the effect of k_{in} on the synchronicity for different scales of driving noise. The results of my simulations can be seen in Fig. 4.1. Here, each line represents a different input noise level and each colour a different k_{in}.

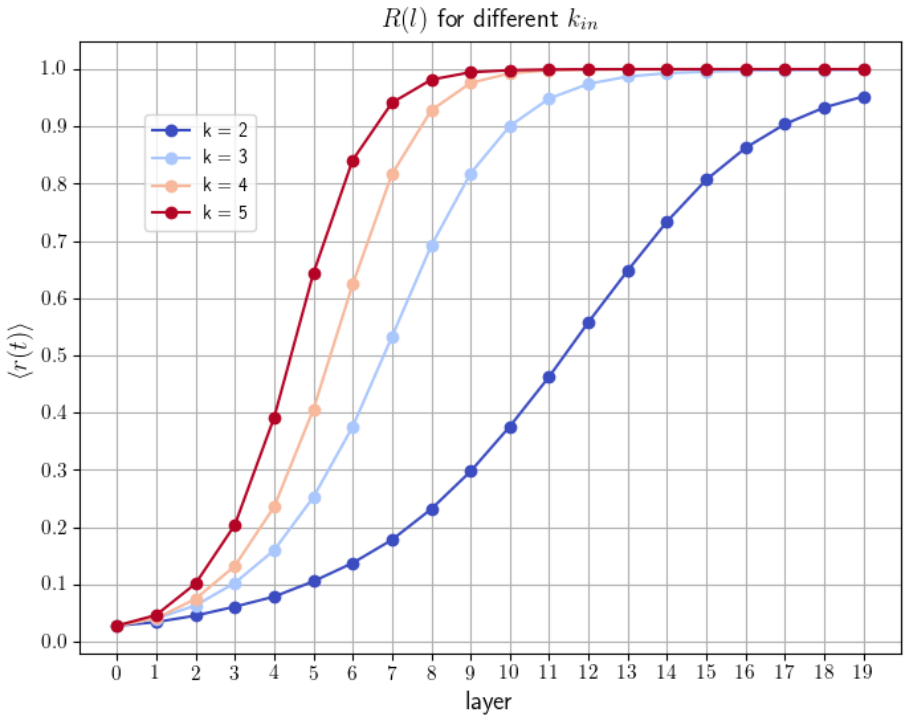

Figure 4.1: Impact of k_{in} on the order of each layer, for a system with 1000 units integrated over a period of 20,000 steps with a size of dt = 0.01.

All the curves in Fig. 4.1 show an accelerating increase up to $R \approx 0.5$ and a subsequent deceleration in climb thereafter, asymptotically approaching $R = 1$ for higher layers. The trend that R increases as l increases, can be explained by the fact, that the oscillators receive inputs from random chains of oscillators in previous layers, resembling a k-ary tree. This means the further away a node is from l=0, the longer and the more branched those chains become. Inputs therefore have more time and ways to mix, each time they do, becoming more and more similar due to the randomness of connections. This leads to later layers receiving increasingly similar inputs from layers before, thus increasing the order within them. It also explains the second trend visible from the graph, where greater input densities cause the layers to begin synchronising closer to $l = 0$. Here, the input chains are able to make additional branches, creating an opportunity for even more inputs to mix. Signals therefore mix sooner and the increase in order progresses much quicker. This is also backed up by the fact that higher input densities lead to synchronisation in similar networks [8].

Now, let us look at the effect of N on the order of each layer and as before repeat this for different levels of driving noise 4.2.

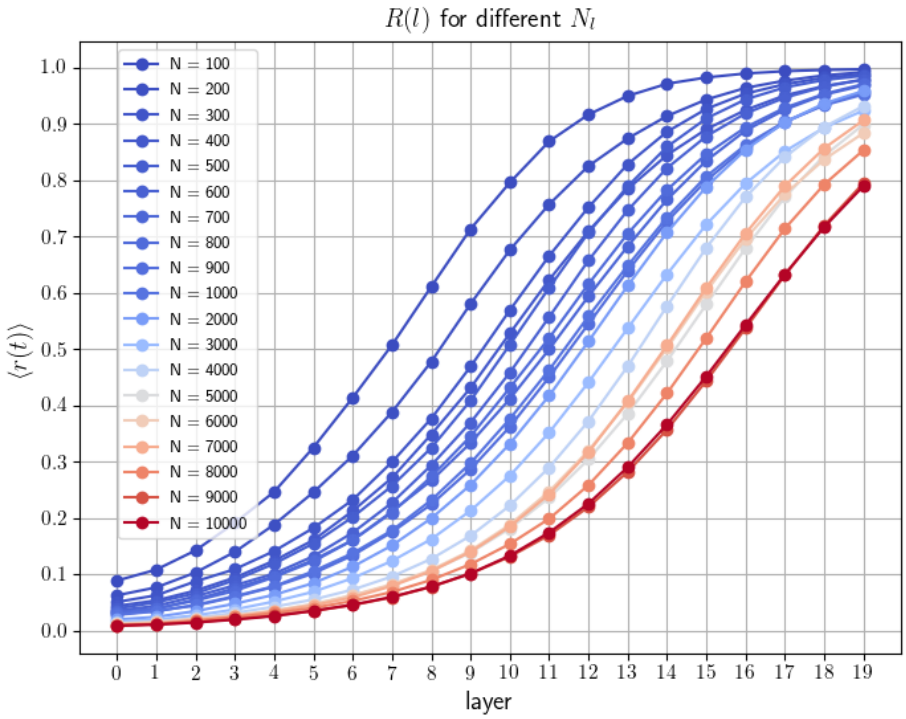

Figure 4.2: Impact of N on the order of each layer, for a system with $k_{in} = 2$ units integrated over a period of 20,000 steps with a size of dt = 0.01.

Here, the shape of the curves looks familiar (compare Fig. 4.1) and order increases again with layer depth. However, across the curves we note, that the higher N the less steep the initial slope is and thus the more sluggish synchronisation. This can be explained by the fact, that even though the number of cross connections stays the same, the number of nodes these can be distributed across is greater. That means, the inputs have more options to mix, causing the effect of mixing overall to be smaller. A higher N therefore is related to a lower order in a given layer.

Lastly, we take a look at the effect of the driving noise parameters on the synchronisation behaviour of each layer. The effect can be seen in Fig. 4.3. I have shaded the graphs according to the magnitude of D_{in} in Fig. 4.3a and γ_{in} in Fig. 4.3b.

The curves are again what we expect from the two previous figures. This time however, across the curves, trends are not nearly as visible, as before. Only a small modulation is visible, with curves staying within a ± 0.2 range of each other on the order scale. Furthermore, the colouration of the plots reveals, that these modulations do not seem to follow any kind of obvious pattern related to

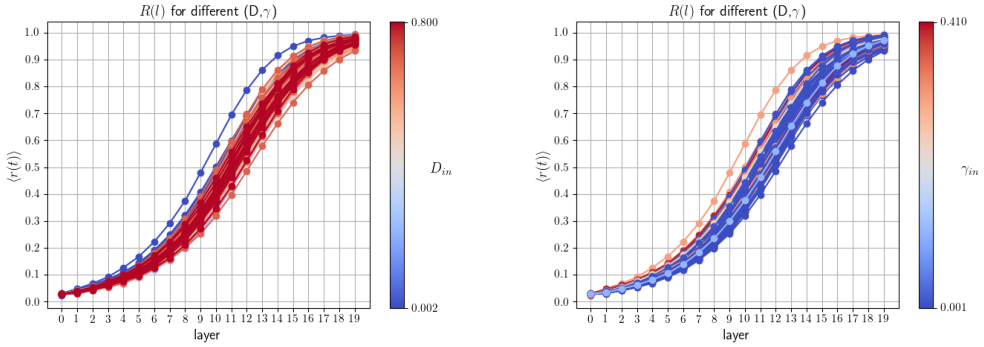

(a) Effect of D_{in} on the order of each layer.

(b) Effect of γ_{in} on the order of each layer.

Figure 4.3: Impact of (D_{in}, γ_{in}) on the order of each layer, for a system with $k_{in} = 2$ units integrated over a period of 20,000 steps with a size of 0.01.

either D or γ individually. The impact of D and γ on the order can therefore be neglected, however one has to be aware, that the effect is non-zero. N and k_{in} should therefore be chosen with this in mind.

To summarise, this implies changing k_{in}, N, D or γ will have an affect on how many layers can be considered asynchronous and thus can be studied. Choosing k_{in}, N, however, is more important than D, γ and they should be chosen in such a way that for all pairs of (D,γ), a sufficient number of layers will be in the asynchronous state. I will therefore restrict myself to studying networks with $2 \leq k_{in} \leq 4$, $N > 1000$ units and $L < 10$ layers. This ensures that $R < 0.5$ for every layer all the time, which guarantees that any measurements made will be made in the incoherent state. I could also use networks of size $N \sim 10^4$ and greater k_{in}, however, this brings an increase in computing time with it that might only in be economically viable in special cases.

4.2 Identifying the Stationary Phase Diffusion Process

Now, that we have identified a parameter region to take our measurements in, lets identify the stationary phase diffusion process, visualise it and look at whether it is unique or not. To do this I will simulate the network behaviour for different sets of driving noises and compare the phase diffusion of the oscillators to a Brownian flight on a circle as outlined in Sec. 2.2.1. An example of this can be seen in Fig. 4.4.

We can see, that the autocorrelation functions show an exponential decay for $\tau\gamma \gg 1$ which is in line with Eq. 2.28. Additionally, the mean circular autocor-

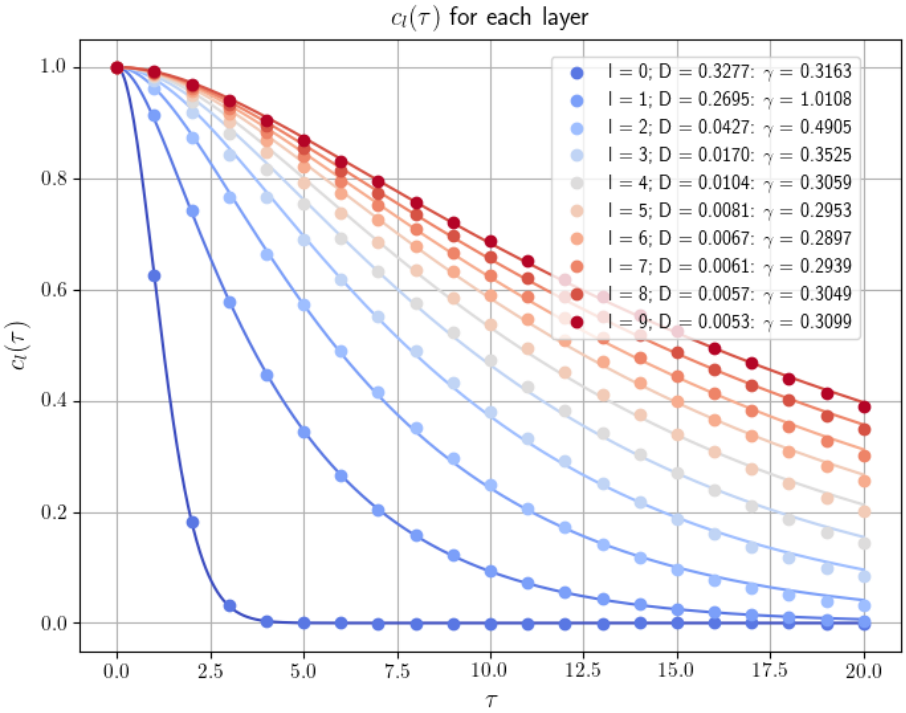

Figure 4.4: Example of the autocorrelation functions for each layer (dots) and the corresponding fits with the autocorrelation function of a Brownian flight on a circle (lines) for a system of 2000 units per layer and 10 layers with $D_{in} = \gamma_{in} = 0.3$.

relation of the oscillators indeed fits the autocorrelation of a Brownian flight on a circle presented in Sec. 2.2.1 very well. This strengthens the case made in this section and confirms our idea about the interactions of the oscillators.

Now, in order to identify the stationary diffusion process, we look at the evolution of D and γ through the layers, plotting graphs for D and γ in relationship to the layer depth. These parameters will be extracted from the fits of the autocorrelation functions with $\tau_{max} = 5$, $\tau_{step} = 0.5$, and a system size of $N_L \cdot L = 2000 \cdot 10$. This way we should be able to see where the parameters characterising this process converge and if they do so for multiple sets of parameters (D_{in}, g_{in}). I will start by covering large ranges of parameters in rough detail, meaning large steps between points in the parameter space and decrease the scope of my measurements around the apparent fixed points, while increasing fidelity. Initially, I will describe the process in detail for $k_{in} = 2$, summarising and discussing results for greater k_{in} only briefly. The results of the first measurements can be seen in Fig. 4.5.

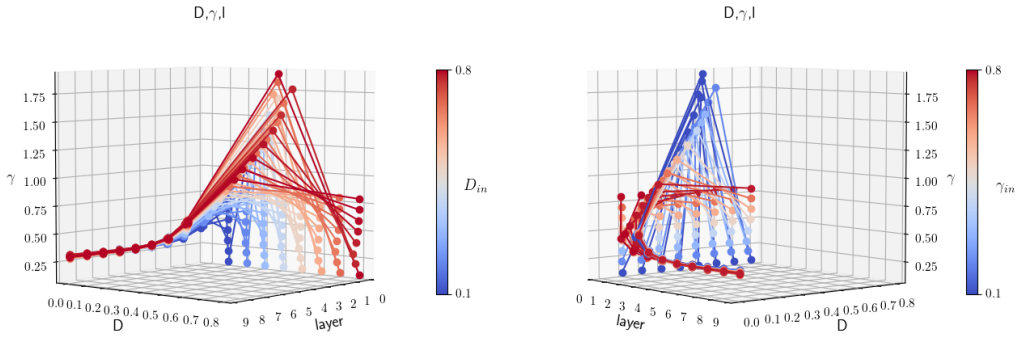

(a) Evolution of D and γ through the layers, for $0.1 \leq D_{in} \leq 0.8$ and $0.1 \leq \gamma_{in} \leq 0.8$ in steps of 0.1, shaded according to the magnitude of D_{in}.

(b) Evolution of D and γ through the layers, for $0.1 \leq D_{in} \leq 0.8$ and $0.1 \leq \gamma_{in} \leq 0.8$ in steps of 0.1, shaded according to the magnitude of γ_{in}.

Figure 4.5: Dependence of the diffusion parameters on layer depth, for a broad range of parameters around the fixed point.

Here and in all subsequent graphs the values D_{in} and γ_{in} denote the preset diffusion parameters of the driving process and $l = 0 \ldots L-1$ the parameters according to the fits for each layer. That means for $l = 0$ the fit parameters might deviate slightly from the preset values, however that is expected, as these values are only in theory reached as $t \to \infty$.

In both graphs we can see that the magnitudes of D and γ change drastically between the first couple of layers. Surprisingly, we see a sharp spike in the value of D in the first layer. The shading in Fig. 4.3a indicates that the lower γ_{in} the higher the spike in the first layer. Further, the shading in Fig. 4.5b shows that the lower D_{in}, also the lower the spike appears. Assuming the trajectories in the bottom corners of Fig. 4.5 approach the fixed point, the closer

D_{in} and γ_{in} to the fixed point, the smaller is the deflection in the first layer.

Generally, this can be explained by the difference in diffusion constants and timescales between the Ornstein-Uhlenbeck process and that of the network. The first layer acts as a kind of buffer between the outside noise and the internal noise. However, with an ever decreasing difference in magnitude between later layers, the change subsides to zero and the graph levels off. Here, the values of D and γ seem to gravitate towards a fixed point. Looking at a sample of trajectories taken from Fig. 4.5 for γ and D separately, the value can already be guessed (Fig. 4.6) to lie about $D \approx 10^{-2}$ and $\gamma \approx 0.3$.

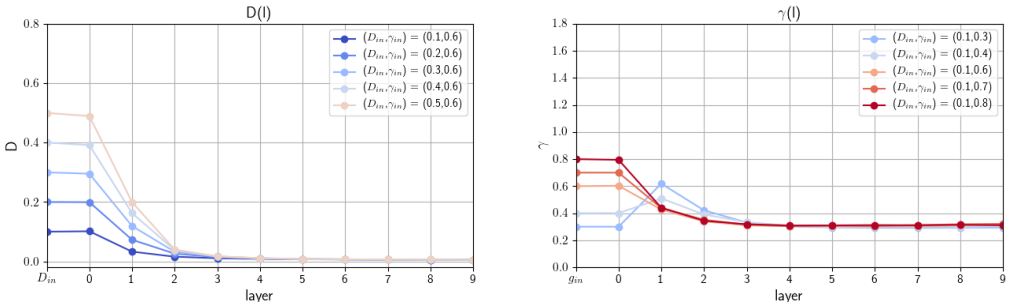

(a) D(l) of for 5 different values of D_{in} at a constant value of γ_{in}.

(b) γ(l) of for 5 different values of γ_{in} at a constant value of D_{in}.

Figure 4.6: Dependence of the diffusion parameters on layer depth, for a broad range of parameters around the fixed point.

Probing closer to those values reveals that our intuition indeed turns out to be true and that we seem to have a fixed point in this region, as the trajectories seem to converge around a narrow band of points as can be seen in Fig. 4.7.

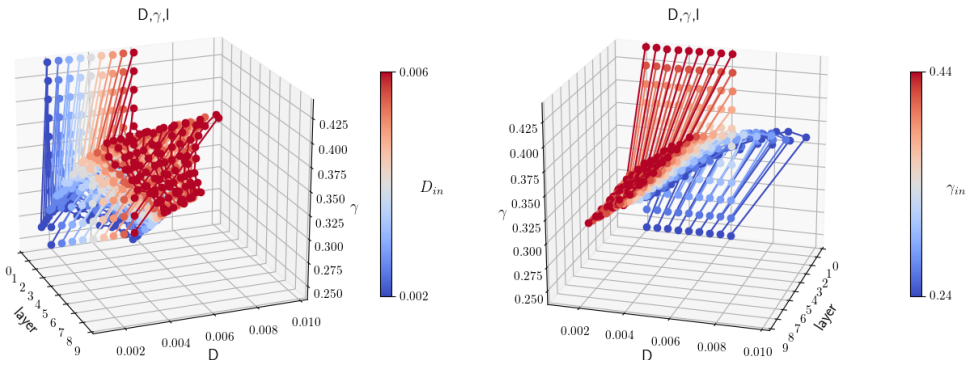

(a) Evolution of D and γ through the layers, for $0.002 \leq D_{in} \leq 0.008$ and $0.22 \leq \gamma_{in} \leq 0.44$ in steps of 0.0005 and 0.02 respectively, shaded according to the magnitude of D_{in}.

(b) Evolution of D and γ through the layers, for $0.002 \leq D_{in} \leq 0.008$ and $0.22 \leq \gamma_{in} \leq 0.44$ in steps of 0.0005 and 0.02 respectively, shaded according to the magnitude of γ_{in}.

Figure 4.7: Dependence of the diffusion parameters on layer depth, for a very small range of parameters around the fixed point.

Here, we can see, that similar to Fig. 4.5, the closer the diffusion parameters are to the estimated fixed point, the less the deflection is in the earlier layers. Furthermore, does the spread of values of our fixed point now lie within the interval $D_{in,min} < D < D_{in,max}$ and $\gamma_{in,min} < \gamma < \gamma_{in,max}$. This would imply, that we could already put bounds around the suspected stationary diffusion process, which indeed we can. Looking at a sample of trajectories taken from Fig. 4.8 for γ and D separately, the value can already be approximated to lie between $0.0039 < D < 0.0042$ and $0.34 < \gamma < 0.36$.

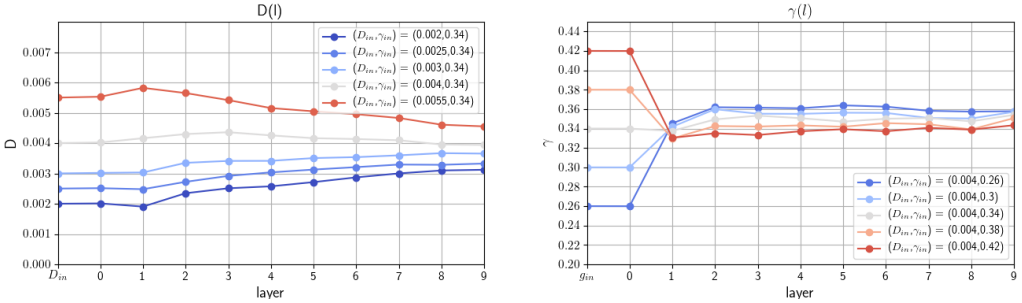

(a) D(l) of for 5 different values of D_{in} at a constant value of γ_{in} close to the suspected fixed point.

(b) γ(l) of for 5 different values of γ_{in} at a constant value of D_{in} close to the suspected fixed point.

Figure 4.8: Dependence of the diffusion parameters on layer depth, for a small range of parameters around the fixed point.

Now, in order to get as rigorous of a measurement as possible for the parameters of the stationary phase diffusion process, I will simulate the system in greater fidelity than before. That means taking finer step sizes than before for D_{in} and γ_{in}. Using larger networks, with 5000 units per layer and 10 layers. Averaging over 5 different realisations of the system. We can then calculate the mean and standard deviations and plot this for every layer, revealing the diffusion and scattering coefficients of the stationary phase diffusion process. This can be seen in Fig. 4.9 and the corresponding table (Tab. 4.1).

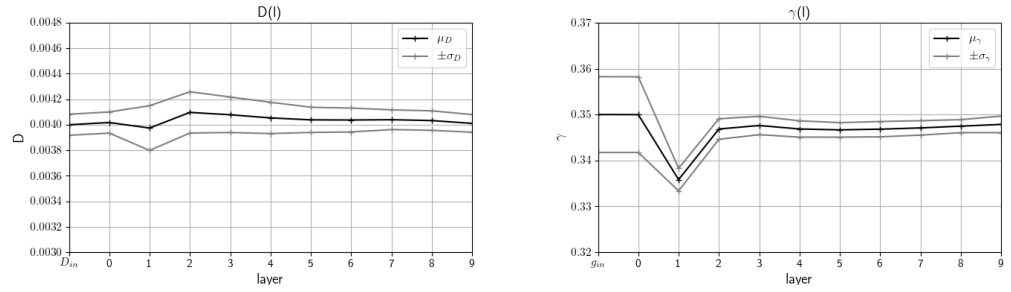

(a) $\bar{D}(l)$

(b) $\bar{\gamma}(l)$

Figure 4.9: Mean and standard deviations of the diffusion parameters for every layer, for a very small range of starting parameters around the fixed point.

layer	$\bar{D}$	σ_D	$\bar{g}$	σ_g
l_0	0.00400	0.00008	0.350	0.008
l_1	0.00402	0.00008	0.350	0.008
l_2	0.00397	0.00018	0.336	0.002
l_3	0.00410	0.00016	0.347	0.002
l_4	0.00408	0.00014	0.348	0.002
l_5	0.00405	0.00012	0.347	0.002
l_6	0.00404	0.00010	0.347	0.002
l_7	0.00404	0.00009	0.347	0.002
l_8	0.00404	0.00008	0.347	0.002
l_9	0.00403	0.00008	0.347	0.001

Table 4.1: Values of $\bar{D}$ and $\bar{g}$ for all layers

Taking the average over all trajectories and points for $l > 4$ (see Fig. 4.10), the fixed point can be estimated to be around

$$\bar{g} = (3.47 \pm 0.02) \cdot 10^{-1}$$
$$\bar{D} = (4.04 \pm 0.09) \cdot 10^{-3}$$

This can also be visualised in the form of a scatter plot for these deeper layers. Every point in a given layer in the graph originates from a different set of input parameters (compare Fig. 4.7).

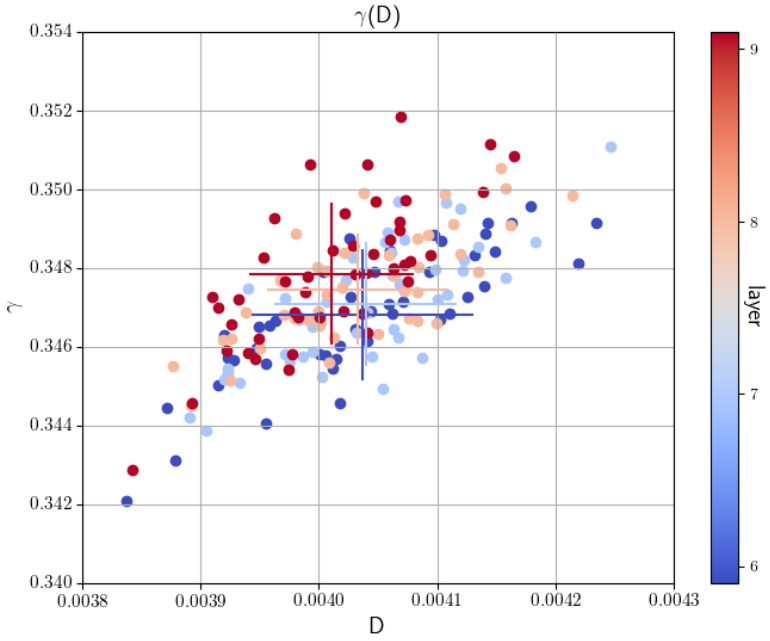

Figure 4.10: The spread of D and γ around the estimated fixed point for different layers, including their means and standard deviations (crosses).

Now, with the stationary phase diffusion process identified for $k_{in} = 2$, for comparisons sake, let us take a look at two more fixed points for higher numbers of k_{in}. For $k_{in} = 3$ and $k_{in} = 4$.

I will make two adjustments compared to the previous simulations, however. Since, for higher numbers of k_{in} the systems synchronise faster, I will simulate fewer layers saving computational resources in the process. Also the later layers tend to synchronise regardless. Secondly, I will use larger systems ($5000 < N < 10,000$) in order to increase connection diversity and thus delay synchronisation as much as possible.

This time I will skip presenting intermediate results of the process, as it is the same as for k_{in} and go right to the last few observations. The results of the processes can be summarised in the following four graphs that can be seen in Fig. 4.11.

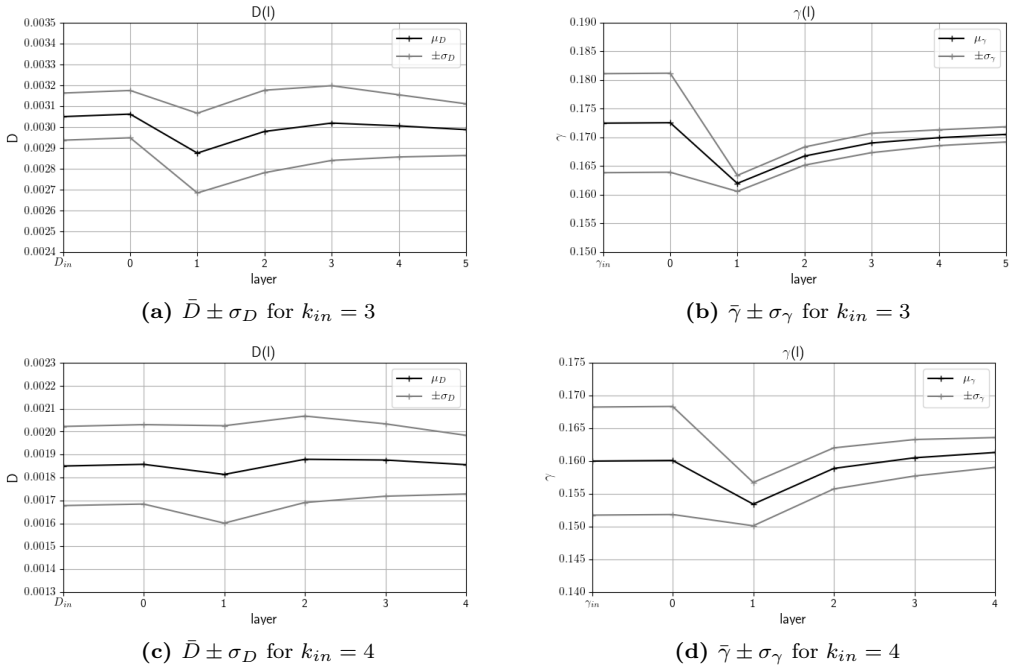

(a) $\bar{D} \pm \sigma_D$ for $k_{in} = 3$

(b) $\bar{\gamma} \pm \sigma_\gamma$ for $k_{in} = 3$

(c) $\bar{D} \pm \sigma_D$ for $k_{in} = 4$

(d) $\bar{\gamma} \pm \sigma_\gamma$ for $k_{in} = 4$

Figure 4.11: Mean and standard deviations of the diffusion parameters for every layer, for a very small range of starting parameters around the fixed point for $k_{in} = 3$ and $k_{in} = 4$.

In all 4 graphs we can see mean and standard deviations for D and γ, which are (magnitude exempted) remarkably similar. While in both cases for k_{in} D stays relatively stable, we notice a similar trend for γ in the first layer, as in Fig. 4.9. Though the dip seems to decrease with k_{in} increasing, it is still present. One might also notice, that compared to Fig. 4.9, it seems to level of more slowly.

This could be due to the fact, that the more incoming connections there are on a given node, the more the local meanfields act like a Brownian process. That means there is a small discrepancy between the driving process in the $0th$ layer and the first driven layer. This would also explain the decrease in the magnitude of the drop with an increase in incoming connections.

Nonetheless, we can use the graphs and the average over the last two (for $k_{in} = 4$) or three (for $k_{in} = 3$) simulated layers to determine the supposed fixed points for these network topologies (see Tab. 4.2).

k_{in}	$\bar{D} \cdot 10^{-3}$	$\sigma_D \cdot 10^{-3}$	$\bar{g} \cdot 10^{-1}$	$\sigma_g \cdot 10^{-1}$
2	4.04	0.02	3.47	0.09
3	3.00	0.15	1.70	0.01
4	1.87	0.14	1.61	0.03

Table 4.2: Values of $\bar{D}$ and $\bar{g}$ for different values of k_{in}

Here, I have summarised all the results from my measurements. We can see, that both D and γ decrease with an increase in k_{in}. It is hard to say what exact trend lies beneath this, just from 3 the data points, however, the decrease between $k_{in} = 2$ and $k_{in} = 3$ for γ_{in} seems to be much more significant, than the when going from $k_{in} = 3$ to $k_{in} = 4$. What this could be caused by, I cannot tell. For this more data would be needed. Possibly with fractions of k_{in}.

5 Conclusions and Outlook

Previous research[8], indicated the existence of a unique stationary phase diffusion process in the incoherent state of a small world network. This lead to the question, if this process can exist in other kinds of homogeneous sparsely connected networks of limit cycle oscillators, specifically in a sparsely connected hierarchical network. I therefore set out to investigate this peculiar behaviour further as part of this thesis. The stated goals were to pinpoint this stationary state, to measure its diffusion parameters and to describe how the network reaches this state.

To do this I created a numerical simulation of the system in question in C++. Here, I implemented an adjustable network and Brownian driving process, as well as functionalities for measuring autocorrelations and order of the system. The latter was of particular significance for the measurement process, since the stationary phase diffusion process, that we were after, is only present in the incoherent state. This meant I first had to determine the ranges of parameters, that allowed the network to settle in a disordered state state. While doing this, I found that the networks order increases with the index of the layers and that it did so unexpectedly quickly. According to my analysis, this points to a strong effect of mixing of inputs, which was unexpected.

Having established the parameter ranges that keep the network in the incoherent state, I could than start with the actual measurements of the phase diffusion processes. Observing the systems reaction to the outside driving noise over extended periods of time, then allowed me to calculate the temporal autocorrelation functions of the individual units. These were subsequently used to gain insight into the phase diffusion process. The was accomplished by using a technique taken from 'Synchronization transition of identical phase oscillators in a directed small-world network'[8], relating the correlation statistics of the individual units to scattering rates and diffusion constants of the underlying phase diffusion process. This enabled me to compare these across the network and with those of the driving process. By simulating the networks behaviour for different ranges of parameters I was then able to show the existence of a

stationary phase diffusion process. Over the ranges of parameters that I have tested - between 0 and 1 for both D and γ - this process seems unique for this type of network and the input densities I looked at. I then went on to determine the location of the fixed points for 3 different densities of inputs. The fixed points can be found at $D = 3.47 \pm 0.02 \cdot 10^{-1}$ and $\gamma = 4.04 \pm 0.09 \cdot 10^{-4}$ for networks with an constant indegree of $k_{in} = 2$. For higher input densities the values decrease and can be found at $D = 3.00 \pm 0.15 \cdot 10^{-4}$, $\gamma = 1.70 \pm 0.01 \cdot 10^{-1}$ and $D = 1.87 \pm 0.14 \cdot 10^{-4}$, $\gamma = 1.61 \pm 0.03 \cdot 10^{-1}$ for $k_{in} = 3$ and $k_{in} = 4$ respectively. The measurements also revealed that there seems to be a great sensitivity for the coupling between the driving process and the first layer of the network to changes in the diffusion parameters around said point.

On a more general note, the results of my experiments show that the described method provides a suitable way to reach, quantify and study the phenomenon of self sustained activity in the incoherent state of hierarchical networks of weakly coupled limit cycle oscillators. Depending on the size and connection density of the network, this is reliably possible for the first number of layers.

Having already quantified the stationary chaotic phase diffusion process for 3 different values of input densities, this opens up the possibility for future work to use the results of my work as a small stepping stone for broader, more detailed numerical studies within the immediate proximity of the fixed point. This could include calculating the power spectra of this state or studying the effect of local or global perturbations, in order to gain better insight into the temporal correlations and their relation to the network. Another idea would be to use not just constant densities of inputs, but distributions and also densities where $k_{in} \in \mathbb{R}$ rather than $k_{in} \in \mathbb{N}$. The hope is that this ultimately might then pave the way for a more analytic description of the chaotic phase diffusion process in this state, which so far has remained a challenging open problem. Understanding the patterns of activity would be a huge step in furthering our understanding of chaotic behaviour in large oscillatory networks, for example enabling the development of more sophisticated models for cortical activity in the brain.

Bibliography

[1] Gyorgy Buzsaki. *Rhythms of the Brain*. Oxford University Press, 2006.

[2] A. Pikovsky, M. G. Rosenblum, and J. Kurths. *Synchronization, A Universal Concept in Nonlinear Sciences*. Cambridge University Press, Cambridge, 2001.

[3] James FA Poulet and Carl CH Petersen. Internal brain state regulates membrane potential synchrony in barrel cortex of behaving mice. *Nature*, 454(7206):881, 2008.

[4] Carl Van Vreeswijk and Haim Sompolinsky. Chaos in neuronal networks with balanced excitatory and inhibitory activity. *Science*, 274(5293):1724–1726, 1996.

[5] Alfonso Renart, Jaime de la Rocha, Peter Bartho, Liad Hollender, Néstor Parga, Alex Reyes, and Kenneth D. Harris. The asynchronous state in cortical circuits. *Science*, 327(5965):587–590, 2010.

[6] Tae-Wook Ko and G. Bard Ermentrout. Partially locked states in coupled oscillators due to inhomogeneous coupling. *Phys. Rev. E*, 78:016203, Jul 2008.

[7] Tae-Wook Ko and G. Bard Ermentrout. Bistability between synchrony and incoherence in limit-cycle oscillators with coupling strength inhomogeneity. *Phys. Rev. E*, 78:026210, Aug 2008.

[8] Ralf Tönjes, Naoki Masuda, and Hiroshi Kori. Synchronization transition of identical phase oscillators in a directed small-world network. *Chaos: An Interdisciplinary Journal of Nonlinear Science*, 20(3):033108, 2010.

[9] Alexander van Meegen and Benjamin Lindner. Self-consistent correlations of randomly coupled rotators in the asynchronous state. *Physical review letters*, 121(25):258302, 2018.

[10] Yoshiki Kuramoto. *Chemical oscillations, waves, and turbulence*. Courier Corporation, 2003.

[11] István Z. Kiss, Yumei Zhai, and John L. Hudson. Predicting mutual entrainment of oscillators with experiment-based phase models. *Phys. Rev. Lett.*, 94:248301, Jun 2005.

[12] G Bard Ermentrout and David Kleinfeld. Traveling electrical waves in cortex: insights from phase dynamics and speculation on a computational role. *Neuron*, 29(1):33–44, 2001.

[13] Hannes Risken. Fokker-planck equation. In *The Fokker-Planck Equation*. Springer, 1996.

[14] Peter E Kloeden and Eckhard Platen. *Numerical solution of stochastic differential equations*, volume 23. Springer Science & Business Media, 2013.

[15] John Wolberg. *Data analysis using the method of least squares: extracting the most information from experiments*. Springer Science & Business Media, 2006.

Statement of Authorship

I herewith declare, that the thesis on hand titled "An Investigation into Self Sustained Activity within a Sparsely Connected Hierarchical Network of Limit Cycle Oscillators in the Incoherent State" has been written without any illegal help of a third party and that all sources have been labeled as such.

Tübingen, 15.10.2019

_____

Jonas Beck